SEMIANNUAL STATUS REPORT

MODELING OF TRANSIENT HEAT PIPE OPERATION

By

Gene T. Colwell
James G. Hartley

Prepared for

NATIONAL AERONAUTICS AND SPACE ADMINISTRATION
LANGLEY RESEARCH CENTER
HAMPTON, VIRGINIA 23665

Under

NASA Grant NAG-1-392

February 1985

GEORGIA INSTITUTE OF TECHNOLOGY
A UNIT OF THE UNIVERSITY SYSTEM OF GEORGIA
SCHOOL OF MECHANICAL ENGINEERING
ATLANTA, GEORGIA 30332

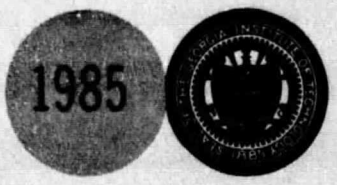

SEMIANNUAL STATUS REPORT

NASA GRANT NAG-1-392

MODELING OF TRANSIENT HEAT PIPE OPERATION

By

Gene T. Colwell and James G. Hartley
School of Mechanical Engineering
Atlanta, Georgia 30332

Submitted to

National Aeronautics and Space Administration
Langley Research Center
Hampton, Virginia 23665

NASA Technical Officer
James C. Robinson
Mail Stop 396

Period Covered
August 19, 1984 through February 18, 1985

February 20, 1985

TABLE OF CONTENTS

INTRODUCTION

This report is intended to summarize progress made on NASA Grant NAG-1-392 during the period August 19, 1984 to February 18, 1985. The overall goal of the project is to gain a better understanding of the transient behiavor of heat pipes operating under both normal and adverse conditions. Normal operation refers to cases where the capillary structure remains fully wetted. Adverse operation occurs when drying, re-wetting, choking, non-continuum flow, freezing, thawing etc. occur within the heat pipe.

The grant was extended for one year on January 1, 1985 and the work was redirected towards developing the capability to predict operational behavior of liquid metal heat pipes used for cooling aerodynamic structures. Of particular interest is the startup of such heat pipes from an initially frozen state such as might occur during re-entry of a space vehicle into the earth's atmosphere or during flight of hypersonic aircraft.

PROGRAM WORK STATEMENT

The program work statement has been changed several times during the past two years. The original long range statement included the following tasks.

I. Compile governing transient equations for heat pipe operation.

II. Model adverse conditions and select non-dimensional groups which can be used to define regimes where adverse operation occurs.

III. Incorporate models for adverse operations into solution techniques. This will involve using thermal property subroutines to predict properties for use in conduction equations.

IV. Assess adequacy of existing finite element computational schemes to handle the models developed.

V. Develop finite element representation of heat pipe for normal operation.

VI. Include non-dimensional groups which define adverse operating regimes in computational scheme.

VII. Select test case to demonstrate techniques.

VIII. Compute operating parameters for test case.

IX. Test computed values against experimental results for test case.

X. Perform parametric studies for system to the extent possible.

XI. Develop, to the extent possible with given time and resources, simplified correlation equations or design procedures.

About one year ago the following tasks were added.

I. Compile a Space Station thermal control candidate technology data base.

II. Develop methodology and algorithms to evaluate candidate technologies.

III. Demonstrate methodology and algorithms through computer-aided assessment example using data base.

The grant was funded for an additional year starting January 1, 1985 and the emphasis was changed to the following tasks.

I. To investigate the physics of melting and freezing of the working fluid in liquid metal heat pipes, and of other performance limitations which are presently not well understood, and to develop equations, adequate for design, to predict associated performance limits.

II. To evaluate the Langley finite difference heat pipe design computer program and the equations upon which it is based and suggest improvements or additions to upgrade the program.

III. To work with the aerospace contractor who wins the heat pipe study contract to upgrade the contractor's heat pipe analysis capability.

IV. To work with NASA to define the required instrumentation for the heat pipe model which will be built under the heat pipe study contract and to develop a test plan for the heat pipe.

While these additions and changes in emphasis in the work statement may at first appear to be excessive, the overall goal has not changed. That goal is to develop predictive techniques for transient heat pipe operation.

EVALUATION OF SPACE STATION THERMAL CONTROL CANDIDATES

A data base is being compiled for candidate technologies for thermal acquisition, transfer and rejection for the Space Station. Representative data were presented in the last progress report. Additional data have been compiled, consolidated and assessed, and typical results are presented in later sections of this report.

During the period covered by this report a computer-aided assessment program was obtained from John B. Hall, Jr. of NASA/Langley Research Center. This program, written in FORTRAN for a Prime Computer, has been installed on the CDC Cyber 180 at Georgia Tech. The installation required a significant number program modifications and was completed in January 1985. Details of the modifications can be provided upon request. The algorithms used for the assessment of candidate technologies have been identified and are currently being evaluated. Examples of the evaluations are discussed in the following paragraphs.

An assessment of candidate data for two thermal acquisition candidates, the conductive cold plate and the two-phase cold plate, has been initiated. The present evaluation is based upon the data in Ref. [1] wherein the design of the internal thermal bus of a space platform is considered. Included in

TABLE 1

Thermal Control Subsystem Heat Loads (after Ref. [1])

Module	Heat Load, kW		
	Metabolic Loop	Equipment Loop	Subsystem Total
Logistics	2.36	1.0	3.36
Habitat	2.36	5.0	7.36
MBA	2.36	6.0	8.36
Lab. No. 1	2.36	10.0	12.36
Lab. No. 2	2.36	30.0	32.36

TABLE 2

Thermal Control Subsystem Weights and Pump Power Requirements for Conductive Cold Plate (after Ref. [1])

Module	TCS Weight, lb			Pump Power, W		
	Metabolic Loop[1]	Equipment Loop[2]	Subsystem Total	Metabolic Loop	Equipment Loop	Subsystem Total
Logistics	69.4	84.0	153.4	21.8	23.8	45.6
Habitat	69.4	226.3	295.7	21.8	102.0	123.8
MBA	69.4	276.0	345.4	21.8	123.0	144.8
Lab. No. 1	69.4	452.0	521.4	21.8	194.0	215.8
Lab. No. 2	69.4	1213.5	1282.9	21.8	566.0	587.8

1. Metabolic loops employ air/water heat exchangers to cool cabin air.

2. Equipment loops employ conductive cold plates for equipment cooling.

the platform are five pressurized modules whose heat loads are summarized in Table 1. The metabolic loops for each module are used to provide temperature and humidity control for the crew metabolic loads by means of air/water heat exchangers. Each module also has cold plates to provide equipment cooling.

CONDUCTIVE COLD PLATE SYSTEM

The following assumptions were made for the conductive cold plate systems analyzed in Ref. [1]:

- The average heat flux density for the conductive cold plate is 270 W/ft^2.
- The cold plate density is 5.3 lb/ft^2.
- The pumping power penalty for the cold plate is 350 lb/kW.
- Water is the working fluid.
- Temperatures at the cold plates are limited to $20 \pm 5^{o}C$.

The total pumping power was determined from a design analysis considering pressure drops throughout the system. Table 2 summarizes the results of the analysis with respect to the weight and pumping power for each of the five pressurized modules. These data and the corresponding loads from Table 1 are presented graphically in Figures 1 and 2. Included in these figures are least squares curve fits which can be incorporated into the computer-aided assessment program. Other candidate data derived from Ref. [1] include the following:

- Cold plate volume (ft^3) = 0.11 * Heat Load (kW)
- Cold plate heat transfer surface area = 3.7 ft^2/kW heat load

TWO-PHASE COLD PLATE SYSTEM

The following assumptions were made for the two-phase cold plate systems analyzed in Ref. [1]:

- The average heat flux density for the two-phase cold plate is 600 W/ft^2.

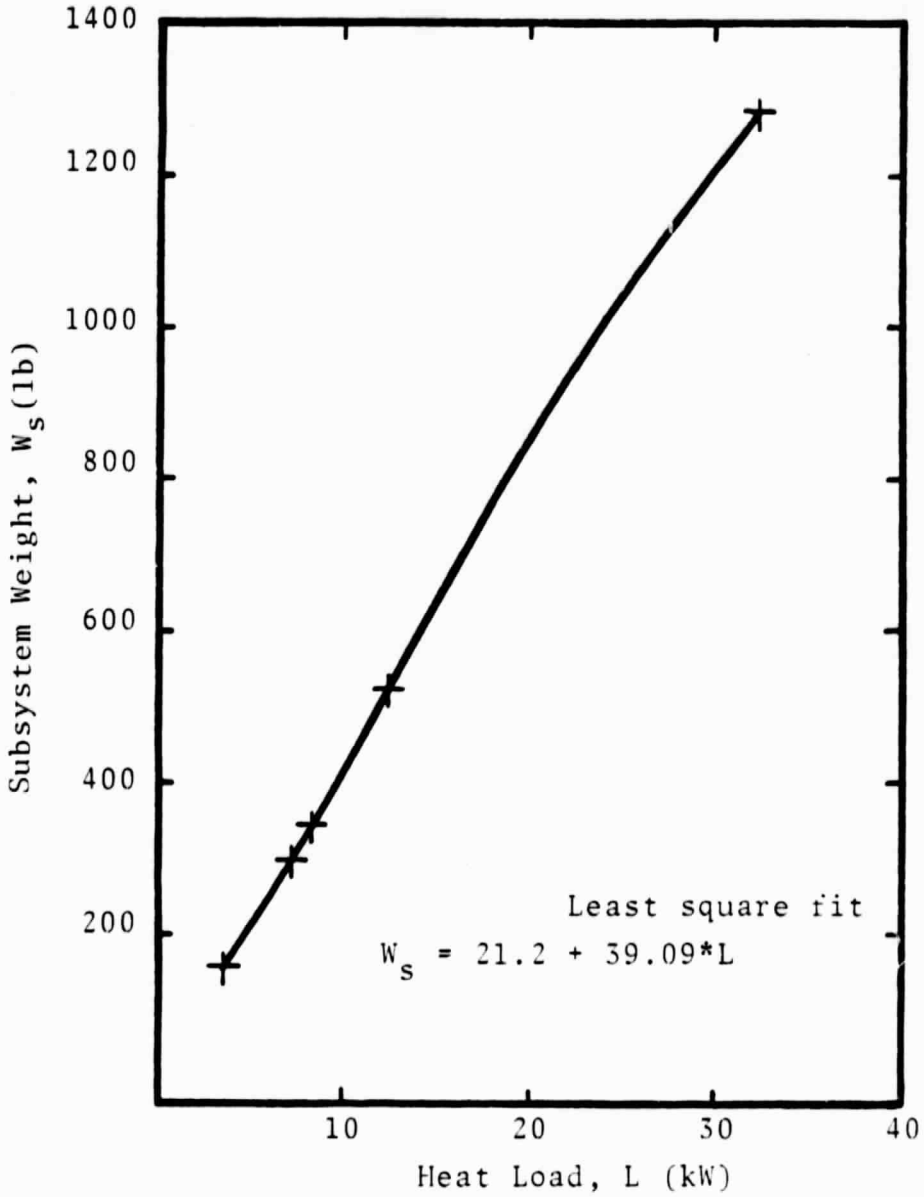

Figure 1. Variation of Subsystem Weight with Heat Load - Conductive Cold Plate System.

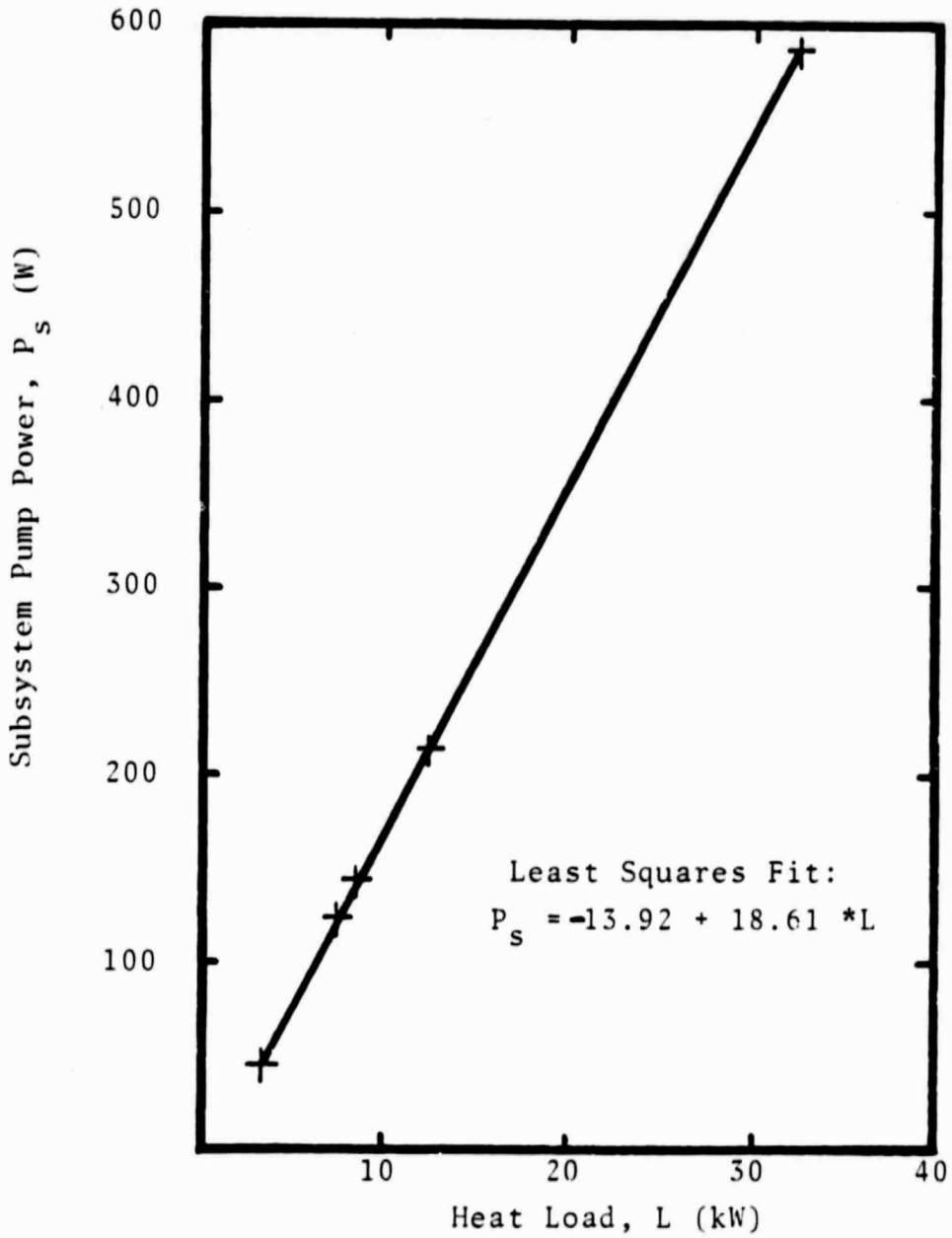

Figure 2. Variation of Subsystem Pump Power with Heat Load - Conductive Cold Plate System.

- The cold plate density is 11.5 lb/ft^2.
- The pumping power penalty for the cold plate is 350 lb/kW.
- Water is the working fluid and complete vaporization occurs in the cold plate.
- Temperatures at the cold plates are limited to $20 \pm 5^{o}C$.

Table 3 summarizes the results of the design analysis from Ref. [1] with respect to the weight and pumping power for each of the five modules. These data and the corresponding loads are presented graphically in Figures 3 and 4. Included in these figures are least squares curve fits which can be incorporated into the computer-aided assessment program. Other data derived from Ref. [1] include the following:

- Cold plate volume (ft^3) = 0.175 * Heat Load (kW)
- Cold plate heat transfer surface area = 1.67 ft^2/kW heat load

COMPUTER IMPLEMENTATION OF CANDIDATE EVALUATION ALGORITHM

The candidate data bases are currently set up for a candidate power rating of 50 kW so that all data are based upon this rating regardless of whether the system is used for thermal acquisition, transport, or rejection. Mission data are used to define the actual power rating, and candidate data are scaled up or down depending upon whether the mission power rating is greater than or less than 50 kW, respectively.

This scheme could be retained for use with new candidate evaluation algorithms. Defining a load fraction,

$$LFRAC = SIZE/50$$

where SIZE is the mission power rating, the pump power required, for example, could be written as

$$P_s = P_s\ (LFRAC)$$

TABLE 3

Thermal Control Subsystem Weights and Pump Power Requirements for Two-Phase Cold Plate (after Ref. [1])

	TCS Weight, lb			Pump Power, W		
Module	Metalbolic Loop[1]	Equipment Loop[2]	Subsystem Total	Metalbolic Loop	Equipment Loop	Subsystem Total
Logistics	91.2	97.1	188.3	0.04	0.01	0.05
Habitat	91.2	198.9	290.1	0.04	0.17	0.21
MBA	91.2	222.2	313.4	0.04	0.26	0.30
Lab. No. 1	91.2	313.9	405.1	0.04	0.34	0.38
Lab. No. 2	91.2	757.5	848.7	0.04	0.86	0.90

1. Metabolic loops employ air/water heat exchangers to cool cabin air.

2. Equipment loops employ two-phase cold plates for equipment cooling.

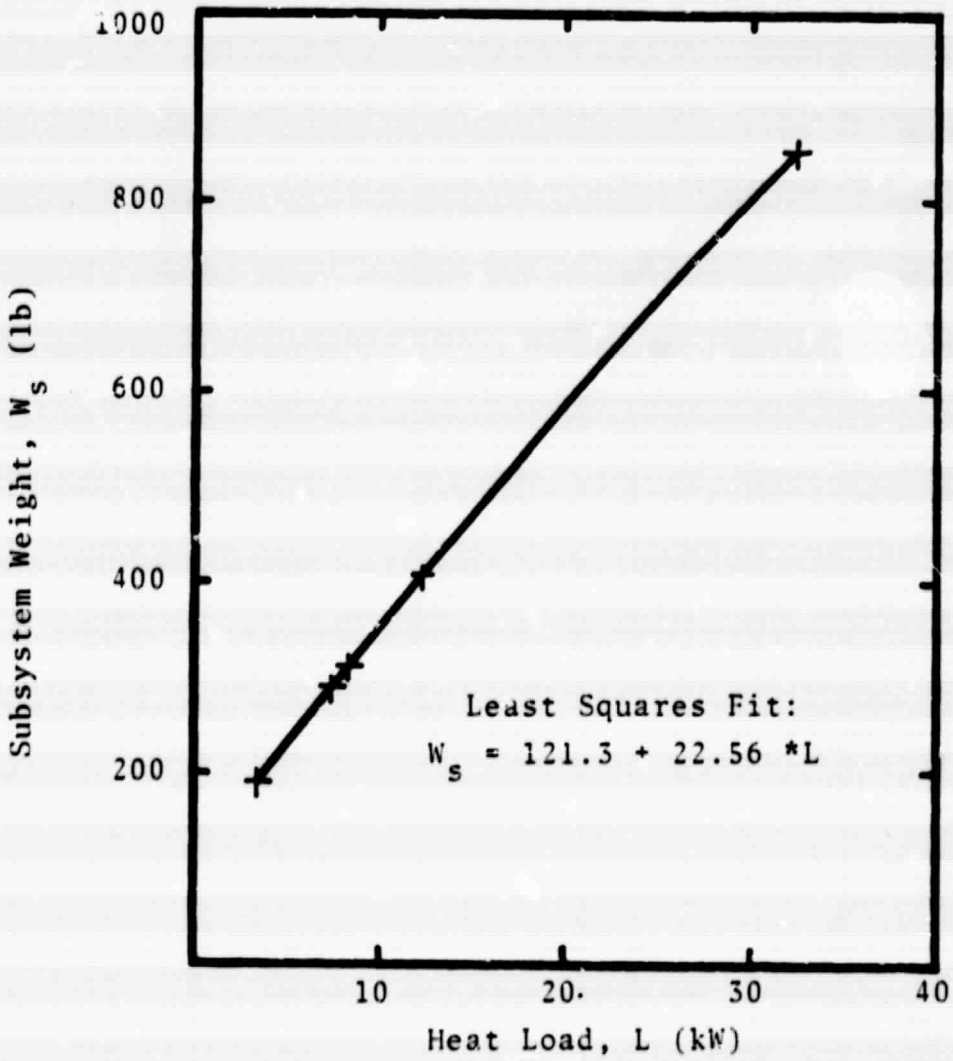

Figure 3. Variation of Subsystem Weight with Heat Load - Two-Phase Cold Plate System.

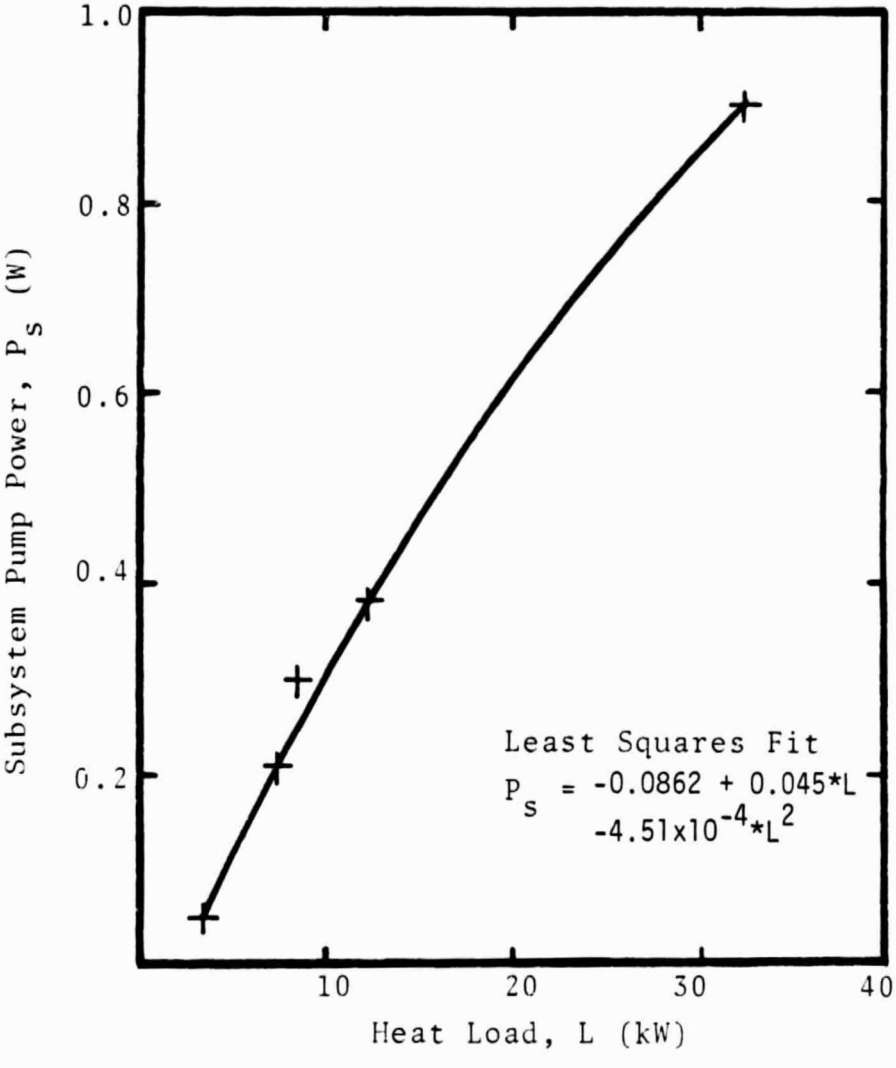

Figure 4. Variation of Subsystem Pump Power with Heat Load - Two-Phase Cold Plant System.

where the function on the left side of this expression is a least squares curve fit of data from the design analysis. The pump power required for the actual mission size could be calculated in the computer-aided assessment program in a number of ways, for example:

Scheme 1 - Add a subroutine or function subprogram which defines P_s = P_s (LFRAC) for each candidate. This would probably be the least flexible means of implementation because the program user could not easily create the subprograms for the various candidates.

Scheme 2 - Store the coefficients of a least squares polynomial curve fit (order $\leq$ 2 should be sufficient) in the data base. This would at least require (a) user input of up to three coefficients used to define P_s(LFRAC) when creation of a data base is desired, (b) larger array sizes for the data arrays used in the program (currently dimensioned to 82), (c) revision of the indexing scheme and dimension for the SYSRAY array in subroutine COMPUTE, (d) revision of the equation used to compute the power required in subroutine COMPUTE; for example,

```
SYSRAY(INDEX+3) = DATARAY(N1,I) + (DATARAY(N2,I) + DATARAY(N3,I)*LFRAC)*LFRAC
```

where N1, N2, N3 are the indices of the array elements containing the coefficients for the least squares polynomial. All other relationships derived from design studies or analyses (i.e. relationships for weight vs. load, volume vs. load, heat transfer surface area vs. load, etc.) could be implemented in a similar manner without much difficulty.

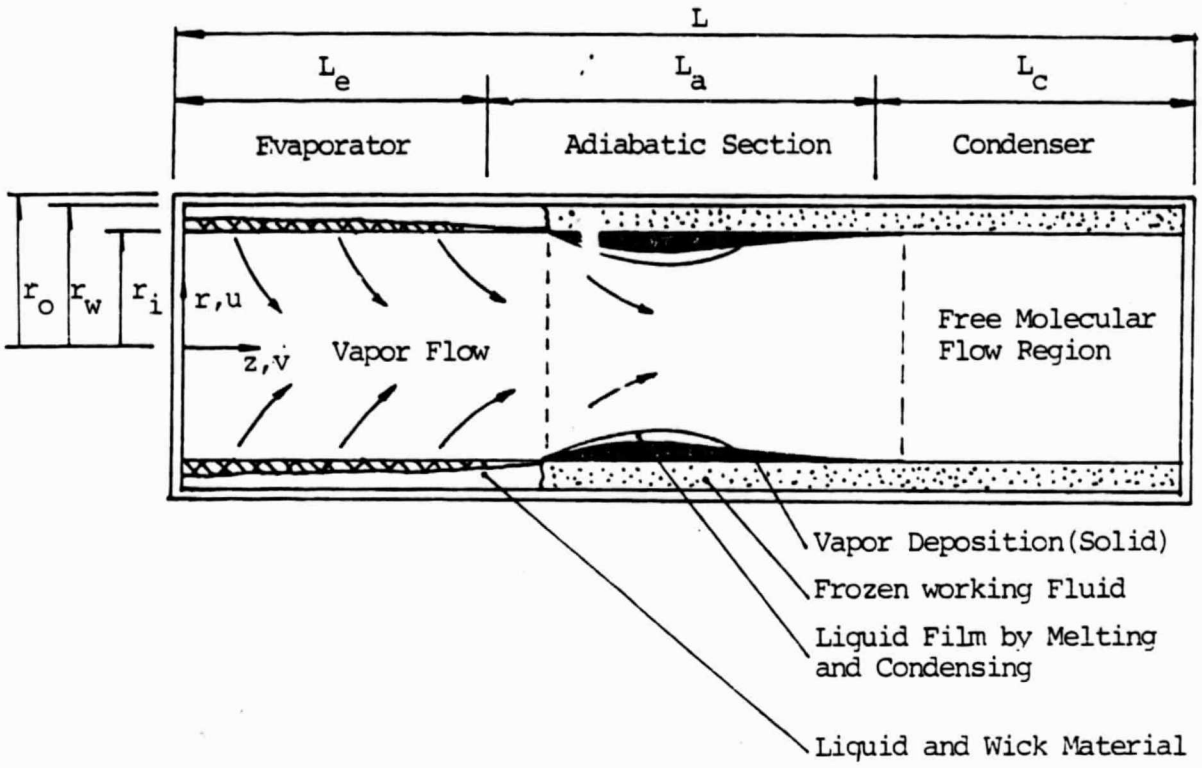

Figure 5. Cylindrical Heat Pipe Model

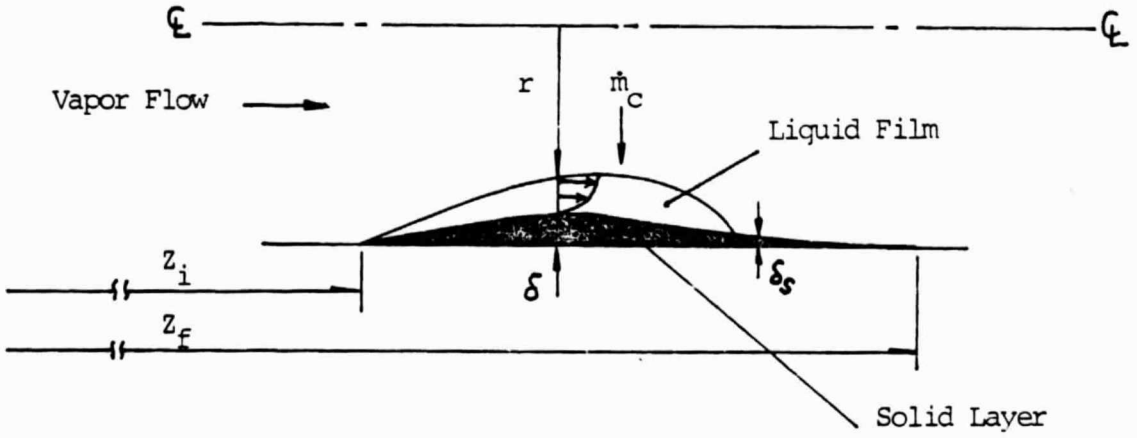

Figure 6 Sketch of the Solid and Liquid Layer

The computer-aided assessment program installed at Georgia Tech is currently being modified along the lines described in Scheme 2 above. Complete details of the required modifications as well as sample assessment results will be reported as soon as they have been completed.

MODELING OF HEAT PIPE STARTUP FORM THE FROZEN STATE

Liquid metal heat pipes experience operating difficulties when a portion or all of the working fluid is solid. Of particular interest, in the utilization of these devices, is startup from an initial state where the working fluid is totally frozen. This problem has been considered by Cotter [2], Ivanovskii et al. [3], Deverall et al. [4], Neal [5], Camarda [6], Silverstein [7] and others. However, no comprehensive experimental or theoretical investigation of the problem has been performed. The goals of the present work, therefore, are to examine the physics of the processes that occur during startup from a frozen state, to mathematically model the processes, to develop numerical techniques for evaluating the mathematical models, and to check the mathematical models and solution techniques against experimental data which will be provided by NASA.

Currently, it is believed that the following sequence of events occurs during startup from a frozen state. Initially the working fluid is solid and the vapor density is extremely low so that molecular flow conditions prevail throughout the heat pipe vapor section. When thermal energy is added in the evaporator section melting of the working fluid begins and energy transport from the heated zone to the adjacent unheated zone proceeds quite slowly via axial conduction through the heat pipe wall and the combination of working fluid and wick structure. However, energy transport by the vapor is negligible.

Since energy is continuously added at the evaporator section, after a time the vapor density in the heated zone is increased so that the mean free path of molecules becomes small compared to the diameter of the vapor passage. Thus, in the hot zone a continuum flow regime is established, and in the cold zone the vapor space is still in free molecular flow. The continuum flow regime grows with time until it reaches the end of heat pipe.

After the frozen working fluid in the evaporator section is melted, evaporation can take place at the liquid-vapor interface and vapor can flow toward the condenser section. Initially vapor generated in the evaporator freezes uniformly on the inner surface of the frozen working fluid in the cold zone. For this stage, energy is transferred as latent heat owing to vaporization in the heated zone and condensation and freezing in the cooled zone.

As long as the entire condensate layer is below the freezing temperature, it remains in a solid state. However, the vapor-solid interface temperature increases as the vapor deposition proceeds until it reaches the melting point. Since the central vapor temperature is above the freezing temperature, further condensation of vapor causes simultaneous melting and condensing at the interface, and a liquid layer appears near the leading edge of the frozen working fluid.

During this part of startup the vapor pressure gradient is large and as shown in Figure 5 the vapor flow passage at the condensing zone has the shape of a converging-diverging nozzle. The velocity of the vapor is so high that the vapor shear acting on the interface between the liquid film and vapor is a major driving force of the liquid film. This liquid film is continuously dragged downstream from the leading edge until the liquid meets a colder temperature to solidify. This annular type flow is assumed to be the dominant

flow pattern of the liquid film existing over the condensing zone. In this case, failure of a heat pipe may occur because freezing of the condensed vapor prevents liquid return to the evaporator.

This process continues until the frozen working fluid is completely melted. When the entire working fluid is finally melted, sufficient liquid is returned to the evaporator and normal transient operation begins. Eventually the heat pipe reaches near isothermal and steady state operation.

On the basis of experimental observations, startup behavior of a frozen heat pipe may be divided into three distinct phases for convenience of analysis.

Phase I: The vapor flow in the heat pipe is in a free molecular regime throughout the vapor space.

Phase II: In the vapor space, a continuum flow regime is established in the heated zone and a continuum flow front moves toward the other end of the heat pipe.

Phase III: Continuum flow exists over the entire heat pipe length in the vapor region.

Phase I Modeling

Heat transfer by the vapor is negligible and heat tranasfer from the heated zone to the unheated zone proceeds quite slowly by conduction only. Hence, conduction can be accepted as the sole transport mechanism. The heat pipe is subcooled and initially has uniform temperature, T_∞. Continuum flow is considered to exist in the vapor space when the temperature of the vapor space is greater than that calculated by the following equation.

$$T_v^* = \frac{15708}{R} \left(\frac{\mu}{\rho D} \right)^2 \qquad (1)$$

when μ, ρ , R and D are viscosity, density, gas constant and diameter of vapor space, respectively.

Heat transfer is governed by the conduction equation written in cylindrical coordinates as follow:

$$\frac{1}{r}\frac{\partial}{\partial r}\left(K_i\, r\,\frac{\partial T_i}{\partial r}\right) + \frac{\partial}{\partial z}\left(K_i\,\frac{\partial T_i}{\partial z}\right) = (\rho c)_i\,\frac{\partial T_i}{\partial t}\,,\quad i = P,\ \ell,\ s \qquad (2)$$

where the subscripts p, ℓ , and s denote the heat pipe shell, liquid region, and solid region, respectively.

At each interface, the temperature and the heat flux are continuous. These boundary conditions are

1. At $r = r_w$ (Interface between the shell and wick)

$$K_p\,\frac{\partial T_p}{\partial r} = K_\ell\,\frac{\partial T_\ell}{\partial r} \quad \text{and} \quad T_p = T_\ell \qquad : \quad \text{liquid region}$$

$$K_p\,\frac{\partial T_p}{\partial r} = K_s\,\frac{\partial T_s}{\partial r} \quad \text{and} \quad T_p = T_s \qquad : \quad \text{solid region}$$

$$T_p = T_s = T_\infty \qquad : \quad \text{subcooled solid region}$$

where T_∞ is the initial temperature.

2. At $r = r_\ell$ (Liquid-solid interface)

$$T_\ell = T_s = T_m \text{ (melting temperature)}$$

From an energy balance at the interface,

$$K_\ell \frac{\partial T_\ell}{\partial r} = \rho_s h_{s\ell} \frac{\partial \delta_s}{\partial t} + K_s \frac{\partial T_s}{\partial r}$$

where δ_s is the position of the liquid-solid interface.

3. At $r = r_\infty(t)$ (forward edge of the solid phase temperature wave)

$$T_s = T_\infty$$

This boundary condition is valid as long as $r_\infty > r_i$. When $r_\infty < r_i$, heat is transferred to the free molecular region.

4. At $z = 0$ and L for all r (i.e. both ends of the heat pipe)

$$\frac{\partial T_p}{\partial z} = 0$$

5. No heat transfer occurs external to the shell at the adiabatic section

$$\frac{\partial T_p}{\partial r} = 0$$

6. The external surface of the shell at the evaporator and condenser sections can be exposed to a heat flux, convection or radiation. Thus

$$K_p \frac{\partial T_p}{\partial r} = h(T_\infty - T_p) + \sigma F(T_\infty^4 - T_p^4) + q''$$

or by conduction alone

$$K_p \frac{\partial T_p}{\partial r} = K_o \frac{\partial T_o}{\partial r}$$

where subscript o stands for surrounding material. However, during Phase I, no heat transfer occurs at the condenser section. Thus

$$\frac{\partial T_p}{\partial r} = 0 \text{ at condenser section}$$

Phase II Modeling

A. Liquid flow in the wick

After the frozen working substance has melted in the evaporator the liquid-vapor meniscus has a more concave surface due to evaporation of working fluid. Thus a pressure gradient is set up and the liquid generated owing to phase change at the liquid-solid interface in the wick flows back to the evaporator through the wick. When the wick is no longer able to supply sufficient liquid, the liquid-vapor interface retreats further into the wick.

The analytical model includes the effects of the rate of change of momentum, surface tension forces, frictional forces in the body of the wick as well as axial variation of static vapor pressure. The following assumptions are made concerning the liquid flow model.

1. The wicking material is isotropic, is of constant thickness, and is initially saturated with a wetting liquid.
2. The liquid flow is axisymmetric, incompressible, laminar, and unsteady. The liquid velocity V_l is uniform across the wick, and has a z component only.
3. The liquid-vapor interface meniscus can be characterized by one radius of curvature at axial location.

4. The temperature of the liquid is a function of z and r, and the kinetic energy and the effect of gravity are neglected.

5. The vapor that evaporates or condenses on the liquid-vapor interfaces has a velocity in the radial direction only.

Application of the principle of conservation of mass for the fluid element shown in Figure 7 yields.

$$\frac{\partial}{\partial t}(m_\ell) = \frac{\partial}{\partial z}(\dot{m}_\ell)dz - \dot{m}_v \tag{3}$$

where

$$\dot{m}_\ell = \rho_\ell A_c V_\ell, \quad m_\ell = \rho_\ell A_c dZ, \quad \dot{m}_v = u_o \rho_v P dZ, \quad A_c = \varepsilon\pi(r_w^2 - r_i^2), \quad P = 2\pi r_i$$

and u_o is the velocity of the vapor. Substitution of these expressions for $\dot{m}_\ell$, m_ℓ, $\dot{m}_v$, A_c, and P into equation (3) yields

$$\frac{\partial r_i}{\partial t} = V_\ell \frac{\partial r_i}{\partial z} - \frac{(r_w^2 - r_i^2)}{2r} \frac{\partial V_\ell}{\partial z} \quad \frac{u_o \rho_v}{\varepsilon \rho_\ell} \tag{4}$$

When the entire wick is saturated, equation (4) becomes

$$\frac{\partial V_\ell}{\partial z} = \frac{2\pi r_i}{A_c} \quad \frac{u_o}{} \quad \frac{\rho_v}{\rho_\ell} \tag{5}$$

The momentum equation in the axial direction for the fluid element in Figure 7 is obtained from Newton's second law with Laplace-Young's equation for capillary forces and Darcy's law for friction force.

$$\sum F_z = M_{z-dz} - M_z + M_v + \frac{\partial}{\partial t}(M)$$

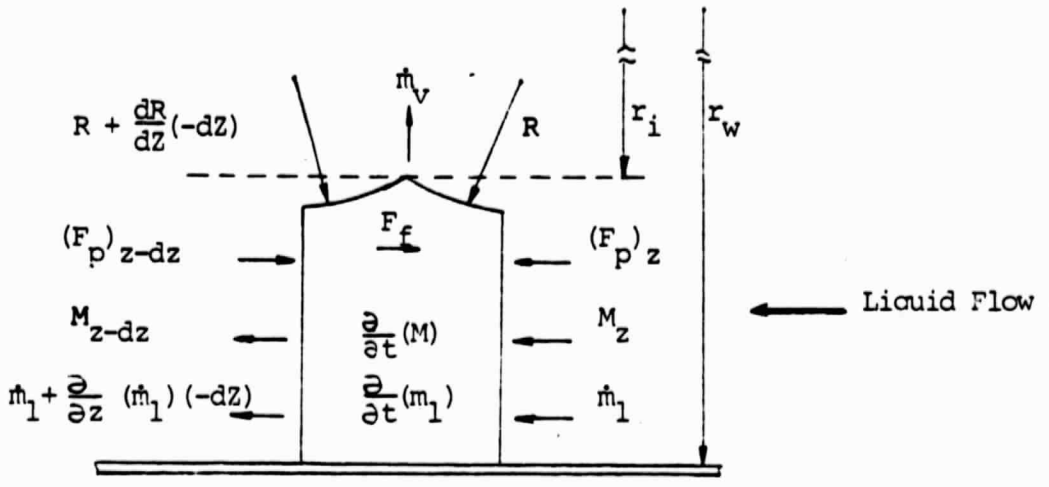

Figure 7. Differential Element of Wick Material for Mass Balance and Momentum Equation.

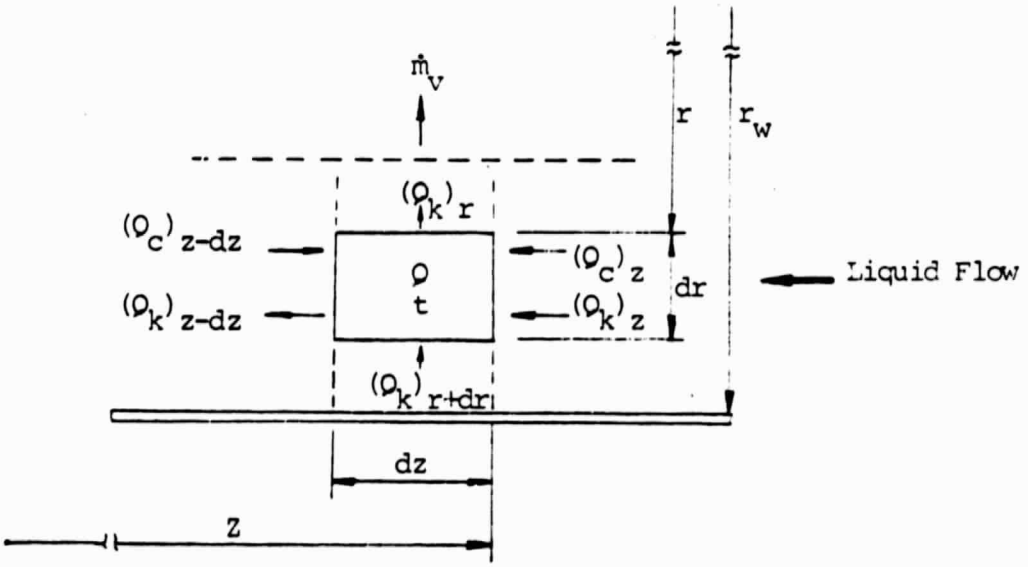

Figure 8. Differential Element of Wick Material for Energy Equation.

or

$$\frac{\partial V_\ell}{\partial t} = V_\ell \frac{\partial V_\ell}{\partial z} - \frac{1}{\rho_\ell}\left[\frac{\partial P_v}{\partial z} - 2\sigma \frac{\partial}{\partial z}\left(\frac{1}{R}\right)\right]$$

$$+ \frac{2r_i}{\rho_\ell(r_w^2 - r_i^2)}\left(P_v - \frac{2\sigma}{R}\right)\frac{\partial r_i}{\partial z} + \frac{\varepsilon}{K_1}\left(\frac{\mu_\ell}{\rho_\ell}\right)V_\ell \qquad (6)$$

where K_1 is the permeability of the wick and σ is liquid-vapor surface tension.

The principle of conservation of energy applied to a differential wick element as shown in Figure 8 yields

$$\frac{\partial}{\partial t}(m_\ell u_\ell) = \frac{\partial}{\partial z}\left(A_c K_e \frac{\partial T_\ell}{\partial z}\right) dz + \frac{\partial}{\partial r}\left(2\pi r K_e \frac{\partial T_\ell}{\partial r} dz\right)dr$$

$$+ \frac{\partial}{\partial z}(\dot{m}_\ell h_\ell)dz \qquad (7)$$

or

$$(\varepsilon\rho_\ell C_v)\frac{\partial T_\ell}{\partial t} = \frac{\partial}{\partial z}\left(K_e \frac{\partial T_\ell}{\partial z}\right) + \frac{1}{r}\frac{\partial}{\partial r}\left(rK_e \frac{\partial T_\ell}{\partial r}\right) + (\varepsilon\rho_\ell C_p)V_\ell \frac{\partial T_\ell}{\partial z}$$

$$+ \frac{\varepsilon}{r}\frac{\partial}{\partial z}(rV_\ell P_\ell) \qquad (8)$$

where K_e is the thermal conductivity of the liquid-wick combination.

Boundary conditions are

1. at $Z = 0$

$$V_\ell = 0 \text{ and } \frac{\partial T_\ell}{\partial z} = 0$$

2. at $r = r_w$ (interface between liquid and tube shell)

$$K_p \frac{\partial T_p}{\partial r} = K_e \frac{\partial T_\ell}{\partial r} \text{ and } T_p = T_\ell$$

3. at $r = r_v$ (liquid-vapor interface)

Boundary conditions will be stated in section B.

4. at $z = z_i$ (liquid-solid interface in wick)

$$r_v = r_i$$

$$V_\ell = \frac{\rho_s}{\rho_\ell} \frac{\partial z_i}{\partial t} \qquad \text{(mass balance)}$$

$$- K_e \frac{\partial T_\ell}{\partial z} = \rho_s h_{s\ell} \frac{\partial z_i}{\partial t} - K_s \frac{\partial T_s}{\partial z} \qquad \text{(energy balance)}$$

$$T_\ell = T_s = T_m \qquad \text{(melting temperature)}$$

B. Vapor flow

It is assumed that the vapor flow is axisymmetric, compressible, and laminar. The vapor flow can be described by the Navier-Stokes equations for a compressible fluid by neglecting body forces and assuming constant viscosity.

Continuity equation

$$\frac{\partial \rho}{\partial t} + \frac{1}{r} \frac{\partial}{\partial r} (r\rho u) + \frac{\partial}{\partial z} (\rho v) = 0 \qquad (9)$$

Momentum equation for the r-direction

$$\rho\left[\frac{\partial u}{\partial t} + u\frac{\partial u}{\partial r} + V\frac{\partial u}{\partial z}\right] = -\frac{\partial P}{\partial r} + \frac{4}{3}\mu\left\{\frac{\partial}{\partial r}\left[\frac{1}{r}\frac{\partial}{\partial r}(ru)\right]\right\}$$

$$+\frac{1}{3}\mu\frac{\partial}{\partial r}\left(\frac{\partial V}{\partial z}\right) + \mu\frac{\partial^2 u}{\partial z^2} \qquad (10)$$

and the z-direction

$$\rho\left[\frac{\partial V}{\partial t} + u\frac{\partial V}{\partial r} + V\frac{\partial V}{\partial z}\right] = -\frac{\partial P}{\partial z} + \mu\left[\frac{\partial^2 V}{\partial r^2} + \frac{1}{r}\frac{\partial V}{\partial r} + \frac{\partial^2 V}{\partial z^2}\right]$$

$$+\frac{1}{3}\mu\frac{\partial}{\partial z}\left[\frac{1}{r}\frac{\partial}{\partial r}(ru) + \frac{\partial V}{\partial z}\right] \qquad (11)$$

Energy equation

$$(\rho c)_v\left[\frac{\partial T_v}{\partial t} + u\frac{\partial T_v}{\partial r} + V\frac{\partial T_v}{\partial z}\right] = \frac{1}{r}\frac{\partial}{\partial r}\left(r K_v\frac{\partial T_v}{\partial r}\right)$$

$$+\frac{\partial}{\partial z}\left(K_v\frac{\partial T_v}{\partial z}\right) \qquad (12)$$

Whether there is a liquid film or not, two different boundary conditions exist in the condensing region. When no liquid film exists

1. at $z = 0$

$$u = 0,\ V = 0,\ \frac{\partial T_v}{\partial z} = 0$$

2. at $r = 0$ (at center of heat pipe)

$$u = 0, \quad \frac{\partial V}{\partial r} = 0, \frac{\partial T_v}{\partial r} = 0$$

3. at $r = r_v$ and $0 \leq z \leq L_e$ (liquid-vapor interface at evaporator)

$$V = 0, \; T_\ell = T_v = T_{sat} = \frac{1}{\frac{1}{T_3} - \frac{R}{h_{\ell v}} \ln \left(\frac{P}{P_3} \right)}$$

where P_3 and T_3 are the pressure and temperature at the triple point.

$$u = - u_o(z,t) = - \frac{1}{\rho_v h_{\ell v}} \left[K_e \frac{\partial T_\ell}{\partial r} \right) - K \frac{\partial T}{\partial r})_v \right]$$

4. At liquid-vapor interface in adiabatic section

$$u = 0, \; v = 0, \; K_e \frac{\partial T_\ell}{\partial r} = K_v \frac{\partial T_v}{\partial r}$$

5. at $r = r_i - \delta_s$ and $z_i \leq z \leq z_f$ (solid-vapor interface)

$$v = 0$$

$$u = u_o(z,t) = \left(\frac{\rho_s}{\rho_v} \right) \frac{\partial \delta_s}{\partial t} = \frac{1}{h_{vs} \rho_v} \left[K_s \frac{\partial T_s}{\partial r} - K_v \frac{\partial T_v}{\partial r} \right]$$

$$T_s = T_v = T_{sub} = \frac{1}{\frac{1}{T_3} - \frac{R}{h_{vs}} \ln \left(\frac{P_3}{P} \right)}$$

6. At the end of continuum flow ($z = z_f$)

$$u = 0, \; V = 0, \; \frac{\partial T_v}{\partial z} = 0$$

If a liquid layer exists on the solid layer, other boundary conditions are needed. These conditions will be stated in the next section.

C. Liquid film

When the temperature at the solid-vapor interface reaches the melting temperature, a thin liquid film is formed over the solid by simultaneous condensing of vapor and melting of solid. The following assumptions are made for mathematical formulation of the model shown in Figure 6.

1. A continuous laminar film exists.
2. Fluid property variations and gravity effects are neglected.
3. The transient and convection terms are neglected in the momentum and energy equation.

Continuity equation

$$\frac{\partial \delta}{\partial t} + \frac{\partial}{\partial z} \left(\int_{r_i - \delta}^{r_i} V_\ell \, dr \right) = \frac{\dot{m}_c}{\rho} \tag{13}$$

Momentum equation

$$\frac{\partial}{\partial r} \left(r \frac{\partial V_f}{\partial r} \right) = 0 \tag{14}$$

Energy equation

$$\frac{\partial}{\partial r} \left(r \frac{\partial T_f}{\partial r} \right) = 0 \tag{15}$$

Boundary conditions

1. at $r = r_i - \delta_s$ (liquid - solid interface)

$$u_f = V_f = 0$$

$$T_f = T_s = T_m \text{ (melting temperature)}$$

$$\frac{\partial \delta_s}{\partial t} = - \frac{1}{h_{s\ell} \rho_s} \left[K_s \frac{\partial T_s}{\partial r} - K_f \frac{\partial T_f}{\partial r} \right]$$

2. at $z = z_i$

$$\delta = \delta_s = 0 \text{ for all time}$$

3. at $z = z_f$

$$\delta_s = 0 \qquad \text{for all time}$$

4. at $r = r_i - \delta$ (liquid-vapor interface)

$$\mu \frac{\partial V}{\partial r})_v = \mu \frac{\partial V}{\partial r})_f \text{ (continuity of shear stress)}$$

$$V_v = V_f \qquad \text{(continuity of velocity)}$$

$$\rho_v \left(V_v \frac{\partial \delta}{\partial z} + u_v \right) = \dot{m}_c$$

$$h_{v\ell} \dot{m}_c = K \frac{\partial T}{\partial r})_f - K \frac{\partial T}{\partial r})_v \text{ (interface energy balance)}$$

D. Solid layer

The governing equation is the same conduction equation that describes the

temperature distribution of the frozen substance in Phase I. Also, boundary conditions have been stated in the previous section.

REFERENCES

1. "High Efficiency Automated Thermal Control Sytem Study - Sytems Preliminary Design Performance Analysis and Specifications - Cabin Thermal Bus," Rockwell International Corp., SSDS4-0075, Report to NASA/LBJ on Contract NAS9-16782, May 1984.

2. T. P. Cotter, "Heat Pipe Start Up Dynamics," Thermionic Conversion Specialist Conference, 1967.

3. M. N. Ivanovskii, V. P. Sorokin, and I. V. Yagodkin, "The Physical Principles of Heat Pipe," Clarenden Press, Oxford, 1982, pp. 155-158.

4. J. E. Deverall, J. E. Kemme, and L. W. Filorschuetz, "Sonic Limitations and Startup Problems of Heat Pipes," LA-4518, 1970.

5. L. G. Neal, "An Analytical and Experimental Study of Heat Pipes," TRW Systems, Jan 1967.

6. C. J. Camarda, "Analysis and Radiant Heating Tests of a Heat-Pipe-Cooled Leading Edge," NASA TN D-8468, August 1977.

7. C. C. Silverstein, "A Feasibility Study of Heat-Pipe-Cooled Leading Edges for Hypersonic Cruise Aircraft," NASA CR-1857, November, 1971.